ACS APPLIED MATERIALS & INTERFACES

RESEARCH ARTICLE

www.acsami.org

A facile method to crystallize amorphous anodized TiO_2 nanotubes at low temperature

Yulong Liao, Wenxiu Que,* Peng Zhong, Jin Zhang, and Yucheng He

Electronic Materials Research Laboratory, School of Electronic and Information Engineering and International Center for Dielectric Research, Xi'an Jiaotong University, Xi'an 710049, Shaanxi, People's Republic of China

ABSTRACT: Anodic growth of TiO_2 nanotubes has attracted intensive interests recently. However, the as-prepared TiO_2 nanotubes are usually amorphous and they generally need to be crystallized by sintering above 450 °C. Here, we report on a facile method to crystallize amorphous anodized TiO_2 nanotubes at a low temperature. We find that, simply by immersing them into hot water, the anodized TiO_2 nanotubes can be transformed from amorphous to crystalline state at a temperature as low as 92 °C. Results indicate that the hot water treatment might be a versatile strategy to crystallize amorphous anodized TiO_2 nanotubes at low temperature. Field-emission scanning electron microscopy, transmission electron microscopy, X-ray diffraction analysis, UV−vis spectroscopy, and Brunauer−Emmett−Teller (BET) analysis via N_2 adsorption are used to characterize the resulting samples. In addition, the TiO_2 nanotubes in powder form are taken as photocatalysts to explore their potential applications. Results indicate that the sample after 35 h of hot water treatment shows the highest photoactivity, which is as efficient as the commercial photocatalyst Degussa P25. The photocatalytic testing results demonstrate that the hot water treatment reported in this study can be an alternative approach to the conventional methods.

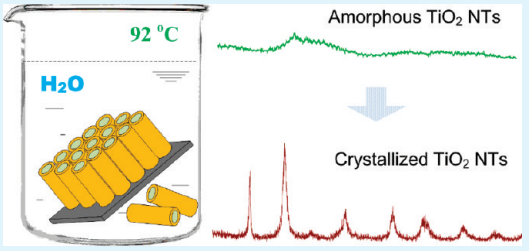

KEYWORDS: TiO_2 nanotube, anodization, hot water treatment, crystalline

1. INTRODUCTION

The size, morphology, geometry, and crystal phase of the nanostructures are important parameters for controlling their chemical, optical, and electrical properties. In light of this, one-dimensional (1D) titanium dioxide (TiO_2) nanotubes (NTs) have attracted a great deal of attentions recently because of their unique properties such as chemical stability, nontoxicity, and high photocatalytic activity.[1−5] As is well-known, TiO_2 is a semiconductor that crystallizes in eight polymorphic forms: rutile (*P*42/*mnm*), anatase (*I*41/*amd*), brookite (*Pbca*), TiO_2-II (*Pbcn*), TiO_2-III (*P*21/*c*), TiO_2-B (*C*2/*m*), TiO_2-R (*Pbnm*), and TiO_2-H (*I*4/*m*). The crystal phase and the composition of the TiO_2 NTs vary with processing techniques and parameters. Titania properties, and hence potential applications, depend on the crystallinity and the isomorph present at the desired operating conditions.[6] For example, rutile phase is preferred in dielectrics and high-temperature oxygen gas sensors,[7,8] whereas anatase phase is mostly used in the area of dye-sensitized solar cells (DSSC) and photocatalysis.[9,10]

Anodic growth of TiO_2 NTs is an effective method to fabricate self-organized TiO_2 NTs due to the simplicity and the high level of geometric control as reported in refs.[9,11−13] Self-organized TiO_2 NTs have been widely used in various applications including photo and thermal catalysis,[14,15] solar cell,[16,17] gas sensing,[18] and marine pollution control.[19,20] However, the as-anodized TiO_2 NTs are usually in the amorphous state and they generally need to be crystallized by sintering above 450 °C before being applied.[6] In the present work, we report on a facile and environmentally friendly strategy to crystallize amorphous TiO_2 NTs at a low temperature (<100 °C). We find that the anodized TiO_2 NTs can be transformed from amorphous state to crystalline state at a temperature as low as 92 °C by immersing them into hot water simply.

In this study, TiO_2 NTs with two types of configuration, namely TiO_2 NT array film and TiO_2 NT powder, were synthesized by electrochemical anodization of titanium sheets. To induce crystallinity, we further treated the NTs with a new strategy called hot water treatment and investigated their morphological and crystalline properties in detail. During the hot water treatment, neither any other additive nor special instrument was required, which was proved to be an alternative method (besides sintering crystallization). Furthermore, the resulting TiO_2 NT powders were taken as photocatalyst to study their performance in the application of photocatalysis.

2. EXPERIMENTAL SECTION

2.1. Preparation of TiO_2 NT Array Film. TiO_2 NT array films were obtained from a starting titanium sheet (0.2 mm thick, 99.6% purity) by potentiostatic anodization in a conventional fluorine containing electrolyte (ethylene glycol containing 0.25 wt % NH_4F and 1.0 wt % deionized (DI) water), using a platinum counter electrode.[9,21] The as-anodized TiO_2 NTs-array films were thoroughly washed with ethanol several times before further treatment. All the reagents were analytical purity and were purchased from Sinopharm Group Chemical Reagent

Received: May 27, 2011
Accepted: June 15, 2011
Published: June 15, 2011

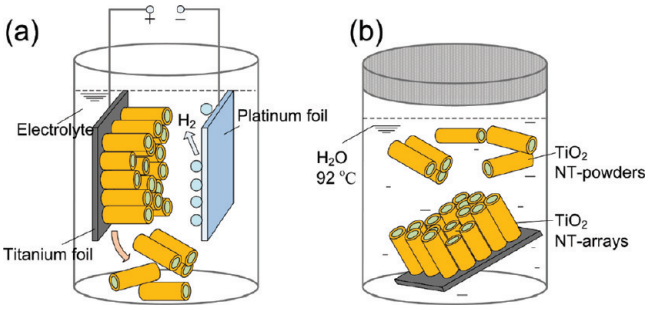

Figure 1. Schematic diagram of (a) the anodization process of Ti sheet into NT-arrays or NT-powders and (b) the hot water treatment process.

Co. Ltd., China. Figure 1a) shows the schematic diagram of the anodization process.

2.2. Preparation of TiO_2 NT Powder. TiO_2 NT-powders were synthesized by a rapid breakdown anodization process in fluoride free electrolytes.[22,23] Briefly, a large piece of Ti foil (4 cm × 4 cm) was directly anodized into the form of the NT powders in 0.15 M $HClO_4$ aqueous solution at room temperature as shown in Figure 1a. After a series of subsequent processing, white TiO_2 NT powders were thus obtained.

2.3. Hot Water Treatment Induced Crystallization. To induce crystallinity, we treated both the as-anodized TiO_2 NT-arrays films and the TiO_2 NTs-powders by the hot water treatment as follows: for the as-anodized TiO_2 NT-arrays films, they were immersed into DI water at 92 °C for 20 h, and then picked them out and allowed them to dry in ambient air. For the as-prepared TiO_2 NT powder, 0.5 g of the TiO_2 NT powders was mixed with 50 mL of DI water, and they were then treated with water bath at 92 °C for 6 h, 11 h, 20 h, or 35 h, respectively. Finally, the resulting powders were separated by centrifugation process and then dried at 60 °C for 12 h. The hot water treatment process was also schematically shown in Figure 1b. For comparison, besides the hot water treatment mentioned above, the as-prepared amorphous TiO_2 NTs were also heated in a furnace (oven dry in air) with the same temperature and duration.

2.4. Characterization. The morphological and structural properties of the TiO_2 anodized NT arrays or powders were characterized by field-emission scanning electron microscopy (FESEM, JSM-7000F, JEOL Inc., Japan) and transmission electron microscopy (TEM, JEM2100, JEOL Inc., Japan). The X-ray diffraction (XRD) patterns of all samples were measured on a D/max-2400 X-ray diffraction spectrometer (Rigaku) with Cu Kα radiation and operated at 40 kV and 100 mA in the 2θ range from 10° to 70°, and the scanning speed was 15° min^{-1} at a step of 0.02°. The UV−vis absorption spectra of the samples were measured under the diffuse reflection mode using a UV−vis-NIR spectrophotometer (Jasco V-570) equipped with an integrating sphere assembly, and the band gap measurements of the as-prepared samples were made using the transformed diffuse reflectance technique according to the Kubelka−Munk theory. The specific surface area of the powders was determined by Brunauer−Emmett−Teller (BET) analysis (Model ASAP 2020, Micromeritics, USA) via nitrogen adsorption at 77 K.

The resulted TiO_2 NT powders were taken as photocatalyst, and their photoactivities were evaluated on the basis of the bleaching of the methyl orange (MO) in an aqueous solution. The sample powder 0.06 g was suspended in MO aqueous solution (100 mL, 20 mg L^{-1}) and irradiated with a 300 W high-pressure mercury lamp. The photodegradation run lasted 40 min, and the samples were taken for examination during the interval of degradation. The concentration of the residual MO solutions was measured by an UV−vis spectrometer (JASCO V-570 UV/vis/NIR). In addition, the as-anodized TiO_2 NTs-powders were sintered at 450 °C for 3 h and the photocatalytic activities of the resulted powders were also tested, which is taken as the control experiment for the photocatalytic testing.

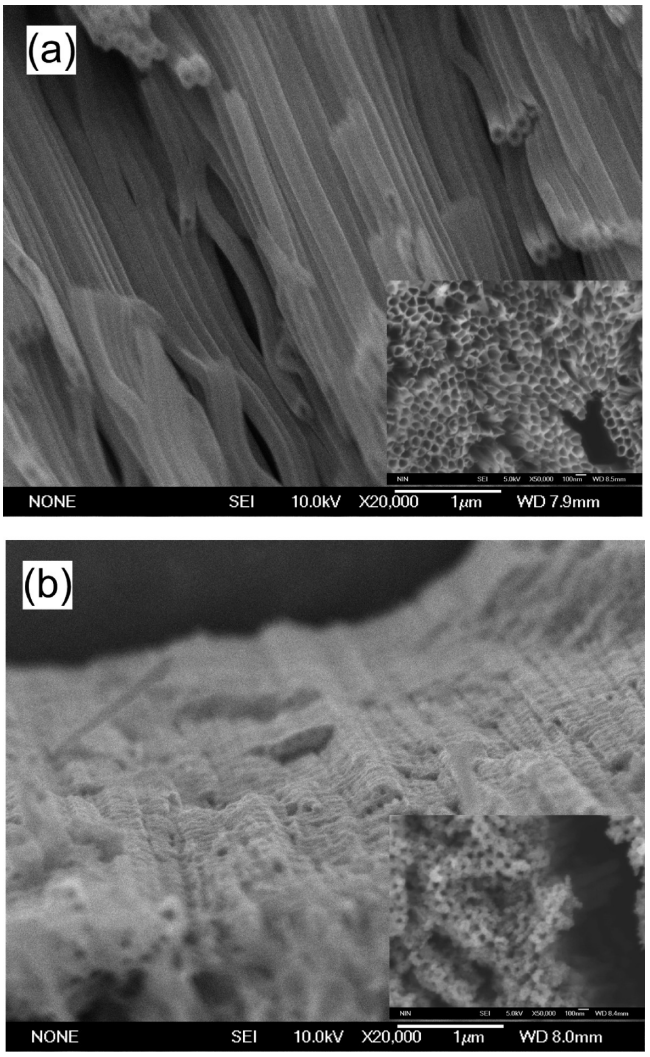

Figure 2. FESEM images of the TiO_2 NT array thin films after (a) oven dry in air and (b) hot water treatment at 92 °C for 20 h.

3. RESULTS AND DISCUSSION

3.1. TiO_2 NT Array Film. Figure 2a shows the FESEM images of the as-anodized TiO_2 NT-array films. It can be seen that the inner diameter of the TiO_2 NT is about 100 nm and the tube length can reach to several micrometers. At the same time, the open mouth and smooth wall of the TiO_2 NTs can be evidently observed. After an oven dry in air at 92 °C for 20 h, the TiO_2 NT array films still hold the same morphologies as the as-anodized sample. However, after the hot water treatment at 92 °C for 20 h, a smooth surface morphology of the nanotube wall disappears, replaced by a rough surface morphology instead as shown in Figure 2b. The rough surface can be attributed to a crystallization of the amorphous TiO_2 NTs induced by the hot water treatment

The crystalline properties of the TiO_2 NT array films were further characterized by XRD and the XRD patterns are shown in Figure 3. It can be seen that only hexagon titanium phase from the substrate is detected before heat treatment, indicating the as-anodized TiO_2 NT array films are still in the amorphous nature.

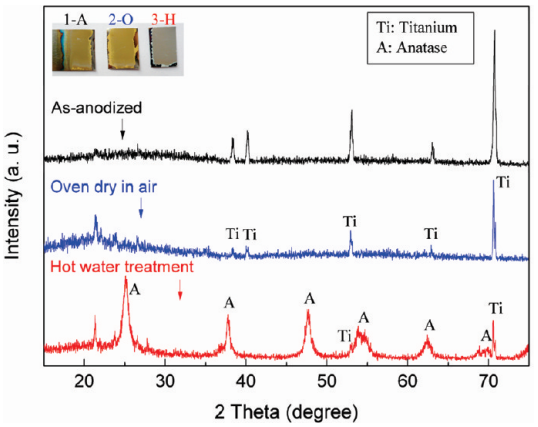

Figure 3. XRD patterns of the TiO_2 NT array thin films after oven dry in air or the hot water treatment at 92 °C for 20 h (1-A, 2-O, and 3-H refer to as-anodized, oven dry in air, and hot water treatment, respectively).

After an oven dry in air at 92 °C for 20 h, the TiO_2 NT array films still hold similar diffraction patterns to the as-anodized samples, which illustrates that there is no any occurrence of the crystallization. Actually, this result consists with the commonly understanding that the anodized TiO_2 NT arrays are stable in amorphous state below 300 °C.[6] When the as-anodized TiO_2 NT array films are heated in water instead, however, strong characteristic peaks of anatase phase can be clearly detected as shown in Figure 3, indicating that the as-anodized TiO_2 NT-array films can be crystallized by using hot water treatment at 92 °C. It can be concluded that the water plays a critical role in the rearrangement processing of the TiO_6^{2-} octahedral from amorphous to anatase. The inset of Figure 3 shows the digital photographs of the TiO_2 NT-array films on titanium substrate, from which their differences in color can be clearly observed. These results are also good in line with what we observed from FESEM.

In conclusion, the anodized amorphous TiO_2 NT array films can be crystallized by the hot water treatment at 92 °C, which is of great importance for the fabrication of the crystallized TiO_2 NT-films on those substrates that cannot sustain a high-temperature treatment. Moreover, the resultant TiO_2 NT arrays own rough surfaces, which actually are of advantages for dye-sensitized solar cells (DSSCs) applications, because the rough surfaces are expected to absorb much more dye molecules.

3.2. TiO_2 NT Powders. Figure 4(a) shows the TEM images of the as-prepared TiO_2 NT-powders by rapid breakdown anodization, indicating the hollow structure and smooth surface of the NTs. The outer diameter and the tube wall thickness are about 20 and 5 nm, respectively, which are coincident with those as reported in refs 22 and 24. After the hot water treatment for 6 h, however, the initial nanotubular structures cannot be observed anymore and the amorphous TiO_2 NTs are transformed into the crystalline state with a crystal grain size of about 10 nm as shown in Figure 4b. With the further growth of these crystal grains, the nanotubular structures of the TiO_2 NT-powders are almost completely destroyed because of the extremely small sizes of the initial TiO_2 NTs (tube wall thickness ~5 nm).

Figure 5 shows the XRD patterns of the TiO_2 NT powders obtained by the hot water treatment with different durations. It can be seen that the amorphous TiO_2 NT powders can transform into a mixed phase of dominant anatase and subordinate brookite

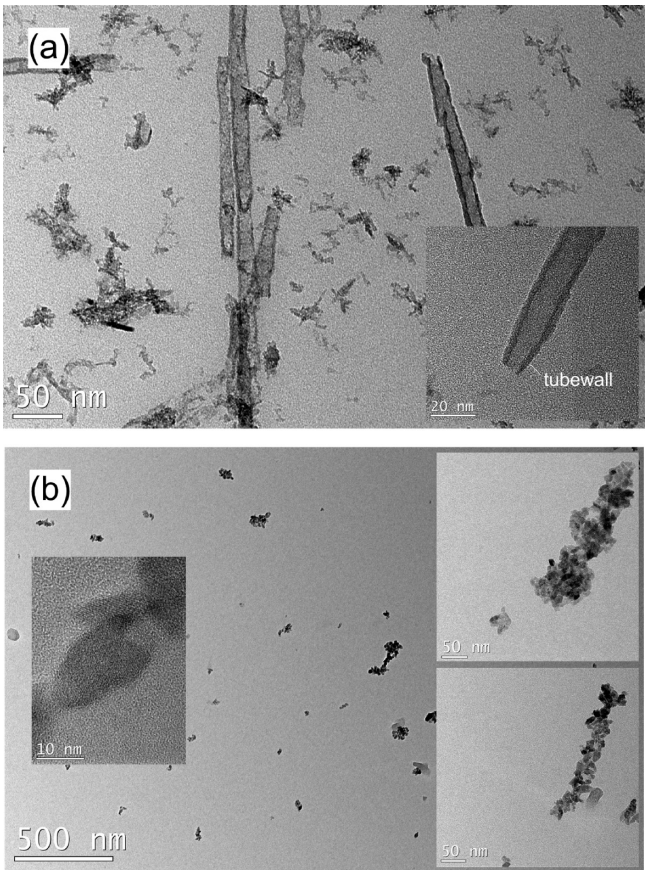

Figure 4. TEM images of (a) the as-prepared TiO_2 NT-powders and (b) the TiO_2 NT-powders obtained after the hot water treatment at 92 °C for 6 h.

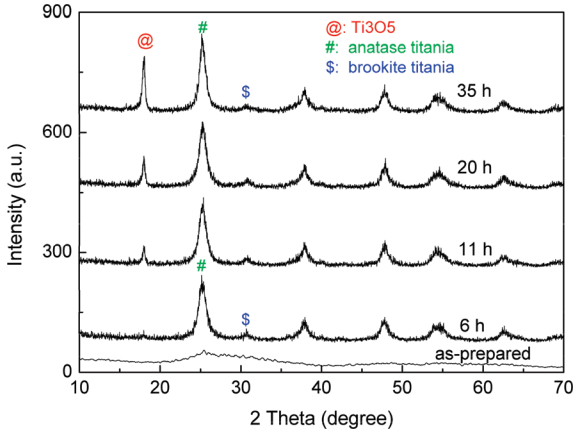

Figure 5. XRD patterns of the TiO_2 NT powders obtained after the hot water treatment at 92 °C under different durations.

after being heated in water for 6 h. According to Debye−Scherrer, the average crystallite size is estimated to be around 8 nm, and it coincides with the TEM observation. When the treatment duration elevates to 11 h, the characteristic peak of Ti_3O_5 (JCPDS pattern no. 23−0606) starts to occur besides the identified peaks of the anatase and brookite. With further increasing treatment duration to 35 h, the resulting powders show a crystalline structure with three-phase (Ti_3O_5/anatase

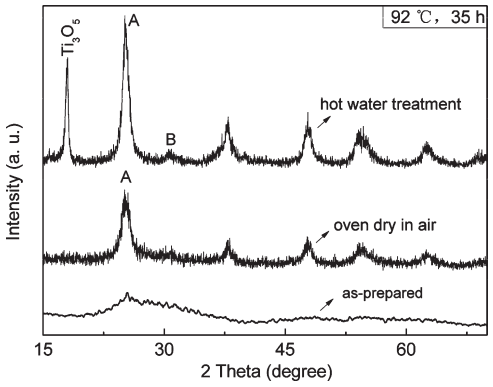

Figure 6. XRD patterns of the TiO_2 NT powders after being treated by different strategies at 92 °C for 35 h (letter A refers to anatase, letter B refers to brookite).

TiO_2/brookite TiO_2). On the basis of the above results, it can be concluded that the TiO_2 NT powders can also be efficiently crystallized by the hot water treatment at a low temperature of 92 °C.

To well-understand the effects of the hot water treatment on the crystallinity of the as-prepared amorphous TiO_2 NT powders, we also heated the as-prepared amorphous TiO_2 NT powders in furnace (oven dry in air). The resulting sample was characterized by XRD as shown in Figure 6. For a convenient comparison, the XRD pattern of the TiO_2 NT powders obtained by the hot water treatment under the same condition (at 92 °C, 35 h) was also included in Figure 6. It can be seen that the TiO_2 NT-powders are only crystallized into an anatase structure after being treated by oven dry in air. However, the sample obtained by the hot water treatment shows a crystalline structure with three-phase of Ti_3O_5/anatase TiO_2/brookite TiO_2. These results indicate that the water is the key factor for the formation of the Ti_3O_5 at low temperature. Generally, there are two mechanisms of crystallization: the solid-state mechanism and the dissolution precipitation mechanism.[25] In present work, it can be seen that the surface of the TiO_2 NT arrays become rougher and the tubular structure of the TiO_2 NT-powders disappear as shown in Figure 2 and Figure 4, respectively, after the hot water treatment. We attribute the crystallization of the amorphous TiO_2 NTs to the dissolution precipitation mechanism. Actually, similar results on the special role of the water in the transformation from amorphous TiO_2 to anatase TiO_2 at low temperature were also reported,[26,27] which occurred only during the sol−gel processes.

As one knows, TiO_2 has been widely studied as photocatalyst. Researchers generally concentrate on two aspects to improve the performance of the photocatalysts: extending the absorption edge and improving the photocatalytic efficiency such as forming anatase/rutile mixed structure. For example, P25 is one of the best photocatalysts among the commercial TiO_2 photocatalysts,[26] and it contains about 85% anatase phase and 15% rutile phase. Here, the Ti_3O_5/anatase TiO_2/brookite TiO_2 nanocomposites are also used as photocatalysts to study their performances in photocatalysis. Figure 7a shows the photocatalytic degradation processing of the MO aqueous solution with the products treated by different strategies. It can be seen form Figure 7a that the sample after sintering at 450 °C for 3 h shows a lower activity than the hot water treated samples. Although the photocatalytic activities of the TiO_2 NT-powders after the hot water treatment increase with

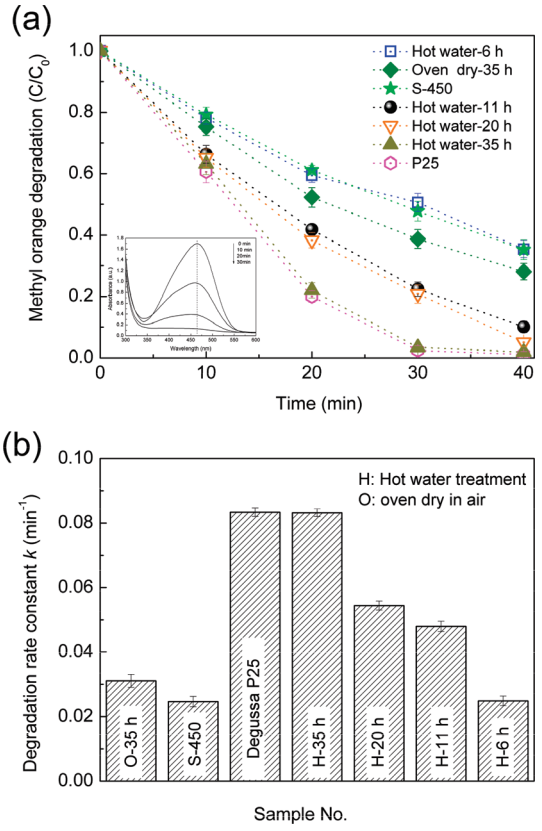

Figure 7. (a) Photocatalytic degradation kinetics of the MO aqueous solution and (b) the degradation rate constant by using the TiO_2 NT-powders obtained under different heat treatment schemes at 92 °C (the inset of (a) shows the MO degradation processing with the TiO_2 NT-powders after hot water treatment at 92 °C for 35 h as photocatalyst, and S-450 refers to the sample sintered at 450 °C for 3 h).

increasing the treatment duration. Especially, the sample after 35 h hot water treatment shows the highest activity among them and can be comparable to the commercial photocatalyst Degussa P25. The MO solution can be almost 100% decompounded within 30 min. As earlier reported, the photocatalytic degradation of the MO aqueous solution can be regarded as a pseudofirst-order reaction,[28] and thereby the degradation rate (k) of all the tested samples in present work were calculated and shown in Figure 7b. It can be seen that the sample after 35 h hot water treatment exhibits a k value as high as that of P25 (~0.082 min^{-1}). BET testing results indicate that the BET specific surface area of the sample after 35 h hot water treatment is about 40.3 $m^2 g^{-1}$, which is actually slightly smaller than that of P25 (~50 $m^2 g^{-1}$).

To further understand the enhancement of the photocatalytic activities, the samples obtained by the hot water treatment were further characterized by UV−vis spectroscopy. It can be found that they have similar UV−vis absorption spectrum and band-gaps of ~3.2 eV (as shown in Figure 8), which indicates that all of them are UV-light photoactive and can absorb similar amounts of photons in the spectrum (<380 nm). Thus, the enhancement of the photocatalytic activity is probably due to the difference in charge separation and recombination. As shown in Figure 5, the crystallinity of the TiO_2 NT-powders is gradually enhanced with the elevation of the treatment duration, indicating the crystalline defects trend to be decreased with the elevation of the treatment duration. Low density of the crystalline defects can reduce the

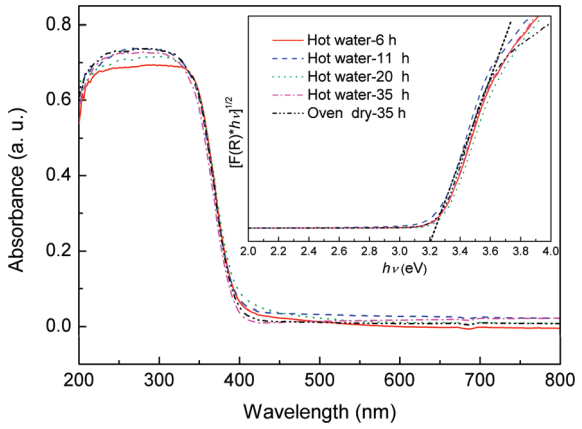

Figure 8. UV−vis absorption spectra of the TiO_2 NT-powders after different heat treatment schemes at 92 °C, and the inset shows the corresponding transformed Kubelka−Munk function vs energy of the excitation source. Determination of the optical band gap is performed by reference to the indirect gap in semiconductors.

recombination of the photogenerated electron−hole pairs.[29] Furthermore, the three-phase (Ti_3O_5/anatase TiO_2/brookite TiO_2) structure can favor the charge separation and thus increase the efficiency of the photocatalysis process.[30] Consequently, the Ti_3O_5/anatase TiO_2/brookite TiO_2 nanocomposites, which are obtained by treating the amorphous TiO_2 NT powders in hot DI water at 92 °C for 35 h, are proved to be an efficient photocatalysts for the photodegradation of the MO aqueous solution. The photocatalytic testing results demonstrate that the hot water treatment reported in this study can be an alternative to the well-documented conventional methods.

4. CONCLUSIONS

We have demonstrated that the amorphous anodized TiO_2 NTs, either in the form of the NT array film or the NT powder, can be crystallized at a temperature as low as 92 °C. By using this hot water treatment strategy, the TiO_2 NT array films and the TiO_2 NT powders can be transformed into anatase phase and Ti_3O_5/anatase/brookite mixed-phase, respectively. The TiO_2 powders, obtained by treating the amorphous TiO_2 NT powder in hot DI water at 92 °C for 35 h, were taken as photocatalysts. They have exhibited as high photocatalytic activities as that of the commercial photocatalyst Degussa P25, indicating that this approach can be an alternative to the well-documented conventional methods. That is to say, the hot water treatment presented in this study shows to be a versatile strategy to crystallize the amorphous anodized TiO_2 NTs at low temperature, which is of great importance and potential applications in many areas.

AUTHOR INFORMATION

Corresponding Author

*Tel.: +86-29-82668679. Fax: +86-29-82668794. E-mail address: wxque@mail.xjtu.edu.cn.

ACKNOWLEDGMENT

This work was supported by the Major Program of the National Natural Science Foundation of China under Grant 90923012, the Ministry of Science and Technology of China through 863-project under Grant 2009AA03Z218 and the Research Fund for the Doctoral Program of Higher Education of China under grant 200806980023.

REFERENCES

(1) Ashid, R.; Morikawa, T.; Ohwaki, T.; Aoki, K.; Taga, Y. *Science* **2001**, *293*, 269.
(2) Bavykin, D. V.; Parmon, V. N.; Lapkin, A. A.; Walsh, F. C. *J. Mater. Chem.* **2004**, *14*, 3370.
(3) Hyett, G.; Darr, J. A.; Mills, A.; Parkin, I. P. *Chem.—Eur. J.* **2010**, *16*, 10546.
(4) Bavykin, D. V.; Walsh, F. C. *Titanate and Titania Nanotubes*; RSC Nanoscience & Nantechnology; Royal Society of Chemisty: Cambridge, U.K., 2009; p 154.
(5) Bavykin, D. V.; Friedrich, J. M.; Walsh, F. C. *Adv. Mater.* **2006**, *18*, 2807.
(6) Varghese, O. K.; Gong, D. W.; Paulose, M.; Grimes, C. A.; Dickey, E. C. *J. Mater. Res.* **2003**, *18*, 156.
(7) Ye, X. S.; Xiao, Z. G.; Lin, D. S.; Huang, S. Y.; Man, Y. H. *Mater. Sci. Eng., B* **2000**, *74*, 133.
(8) Gao, L.; Li, Q.; Song, Z.; Wang, J. *Sens. Actuators, B* **2000**, *71*, 179.
(9) Mor, G. K.; Shankar, K.; Paulose, M.; Varghese, O. K.; Grimes, C. A. *Nano Lett.* **2005**, *5*, 191.
(10) Lai, Y. K.; Zhuang, H. F.; Sun, L.; Chen, Z.; Lin, C. J. *Electrochim. Acta* **2009**, *54*, 6536.
(11) Wang, J.; Lin, Z. Q. *J. Phys. Chem. C* **2009**, *113*, 4026.
(12) Wang, J.; Zhao, L. V.; Lin, S. Y.; Lin, Z. Q. *J. Mater. Chem.* **2009**, *19*, 3682.
(13) Wang, J.; Lin, Z. Q. *Chem. Mater.* **2010**, *22*, 579.
(14) Bavykin, D. V.; Lapkin, A. A.; Plucinski, P. K.; Torrente-Murciano, L.; Friedrich, J. M.; Walsh, F. C. *Top. Catal.* **2006**, *39*, 151.
(15) Torrente-Murciano, L.; Lapkin, A. A.; Bavykin, D. V.; Walsh, F. C.; Wilson, K. *J. Catal.* **2007**, *245*, 272.
(16) Vlachopoulos, N.; Liska, P.; Augustynski, J.; Graetzel, M. *J. Am. Chem. Soc.* **1988**, *110*, 1216.
(17) Foong, T. R. B.; Shen, Y. D.; Hu, X.; Sellinger, A. *Adv. Funct. Mater.* **2010**, *20*, 1390.
(18) Coakley, K. M.; Liu, Y.; McGehee, M. D.; Frindell, K. L.; Stucky, G. D. *Adv. Funct. Mater.* **2003**, *13*, 301.
(19) Lai, Y. K.; Chen, Y. C.; Tang, Y. X.; Gong, D. G.; Chen, Z.; Lin, C. J. *Electrochem. Commun.* **2009**, *11*, 2268.
(20) Ding, S.; Chen, J. S.; Wang, Z.; Cheah, Y. L.; Madhavi, S.; Hu, X.; Lou, X. W. *J. Mater. Chem.* **2011**, *21*, 1677.
(21) Gong, W.; Paulose, M.; Grimes, C. A.; Dickey, E. C. *J. Mater. Res.* **2003**, *18*, 156.
(22) Fahim, N. F.; Sekino, T. *Chem. Mater.* **2009**, *21*, 1967.
(23) Jha, H.; Hahn, R.; Schmuki, P. *Electrochim. Acta* **2010**, *55*, 8883.
(24) Liao, Y.; Que, W. *J. Alloys Compd.* **2010**, *505*, 243.
(25) Yanagisawa, K.; Ovenstone, J. *J. Phys. Chem. B* **1999**, *103*, 7781.
(26) Li, S.; Ye, G.; Chen, G. *J. Phys. Chem. C* **2009**, *113*, 4031.
(27) Matsuda, A.; Higashi, Y.; Tadanaga, K.; Tatsumisago, M. *J. Mater. Sci.* **2006**, *41*, 8101.
(28) Abdullah, A. Z.; Ling, P. Y. *J. Hazard. Mater.* **2010**, *173*, 159.
(29) Amano, F.; Mahaney, O. O. P.; Terada, Y.; Yasumoto, T.; Shibayama, T.; Ohtani, B. *Chem. Mater.* **2009**, *21*, 2601.
(30) Zhang, J.; Zhu, H.; Zheng, S.; Pan, F.; Wang, T. *ACS Appl. Mater. Interfaces* **2009**, *1*, 2111.